RSC Advances

PAPER

View Article Online
View Journal | View Issue

Check for updates

Cite this: *RSC Adv.*, 2020, **10**, 4110

A new bio-compatible Cd^{2+}-selective nanostructured fluorescent imprinted polymer for cadmium ion sensing in aqueous media and its application in bio imaging in Vero cells

Taher Alizadeh, * Amir Reza Sharifi and Mohammad Reza Ganjali

Cadmium is a very toxic element found in various aqueous samples. The majority of the highly selective fluorescent ligands, designed for cadmium ion sensing, are hydrophobic compounds, thus making them inactive in aqueous media. Fluorescent imprinted polymers, synthesized by the proficient combination of hydrophilic functional monomers and hydrophobic ligands, may give a new and highly selective opportunity for utilizing most fluorescent ligands for toxic metal ion sensing in aqueous media. A novel fluorescent Cd^{2+}-imprinted polymer was synthesized based on the co-polymerization of a mixture of acryl amide, vinyl benzene and ethylene glycol dimethacrylate in the presence of a 5-((3-hydroxynaphthalen-2-yl)methylene)pyrimidine-2,4,6(1,3,5)-trione (HMPT)-Cd^{2+} complex. The polymer was characterized by FT-IR spectroscopy, scanning electron microscopy and thermogravimetric analysis. Cadmium ion recognition by IIP created a new emission peak at about 502 nm based on the ICT mechanism, which was different from the emission peak of IIP in the absence of Cd^{2+} (440 nm). The non-imprinted polymer showed a fluorescence emission at about 500 nm, which was not affected by Cd^{2+}, highlighting the recognition sites of IIP. The opto-sensor (IIP) exhibited a dynamic linear response range of 10–0.05 μM with the limit of detection (LOD) and quantification (LOQ) of 12.3 and 41 nM, respectively. Also, the relative standard deviation (RSD) of 3 separate determinations was 3.68%. Moreover, the developed chemosensor was highly selective for Cd^{2+} since the IIP fluorescence was not affected by the presence of other metal ions such as Zn^{2+}, Cu^{+}, Mn^{2+}, Co^{2+}, Ni^{2+}, and Pb^{2+}. The synthesized IIP can be used as a fluorescent probe for cadmium detection in live cells because of its minor cytotoxic effect on them.

Received 30th August 2019
Accepted 21st December 2019

DOI: 10.1039/c9ra06910k

rsc.li/rsc-advances

Open Access Article. Published on 24 January 2020. Downloaded on 2/11/2026 3:01:44 PM.
This article is licensed under a Creative Commons Attribution-NonCommercial 3.0 Unported Licence.

Introduction

Cadmium is a highly toxic metal traditionally found in industrial work places. It has been categorized as one of the 13 most toxic metals by the U.S. Environmental Protection Agency (EPA).[1,2] The allowed limit of cadmium for human consumption in water is about 10 μg L^{-1}.[3,4] It is well-known that exposure to cadmium ions has a ruinous impact on the heart, lungs, bones and particularly kidneys. It is collected in kidneys for several years and disrupts their filtering performance.[5] Therefore, the identification and determination of cadmium ions in various environmental, food and industrial samples are very important.

Different methods such as flame atomic absorption spectrometry (FAAS),[6] inductively coupled plasma atomic emission spectrometry (ICP-AES),[7] inductively coupled plasma mass spectrometry (ICP-MS),[8] spectrophotometry,[9,10] voltammetry,[11–13] potentiometry,[14] chemiluminescence,[15] and atomic[16] and molecular fluorescence spectroscopy[17–19] have been reported for cadmium ion monitoring in various samples.

The development of fluorescent sensing materials has attracted a great deal of attention because of intrinsic sensitivity, simplicity and real-time detection. However, only a few cadmium ion fluorescent sensors have been reported so far.[20–22] The main challenge for Cd^{2+} detection by the molecular fluorescence method is the interference effect of some transition metal ions, especially Zn^{2+}, which belongs to the same group and shows similar characteristics.[23] This means that both Zn^{2+} and Cd^{2+} give rise to similar spectral changes when interacting with the fluorescent ligand.[24–26] Hence, the development of Cd^{2+} selective fluorescent sensors capable of distinguishing Cd^{2+} from Zn^{2+} and other metal ions is an important research field. However, the majority of the complexing agents synthesized for the fluorescence sensing of toxic metal ions are hydrophobic materials, making them inappropriate for applications in aqueous solutions for sensing and determination.[27–32]

Department of Analytical Chemistry, Faculty of Chemistry, University College of Science, University of Tehran, P. O. Box 14155-6455, Tehran, Iran. E-mail: talizadeh@ut.ac.ir

This journal is © The Royal Society of Chemistry 2020

Open Access Article. Published on 24 January 2020. Downloaded on 2/11/2026 3:01:44 PM.
This article is licensed under a Creative Commons Attribution-NonCommercial 3.0 Unported Licence.

Molecularly imprinted polymers (MIPs) are introduced in sensing applications as tailor-made sensing materials and have received great attention due to their fascinating characteristics such as high selectivity, chemical and mechanical stability and ease of fabrication. They are usually synthesized by utilizing the covalent or non-covalent interaction between print molecules and functional monomers in the presence of a cross-linker to fabricate a three-dimensional polymer. After template removal from the polymer, selective sites complementary in size, coordination geometry, and coordination number to the target molecules are created within the polymer.[33–35] In a parallel approach, ion-imprinted polymers (IIPs) are similar to MIPs except that ionic species are trapped in the polymer structure during the synthesis process.[36–40]

Fabricating fluorescent ion-imprinted polymers is still a challenging task since most of the metal ions have no fluorescence characteristics. Despite this, several fluorescent metal ion-imprinted polymers have already been reported.[41–44] One interesting aspect of fluorescent imprinted polymers is that it provides an opportunity to combine hydrophobic fluorescent ligands with the hydrophilic structure of the cross-linked polymer, thus enabling the resulting material to be used for metal ion sensing in aqueous media because fluorescent ligand-loaded IIP can be effectively dispersed in water samples to recognize target ions.

This study concentrated on the synthesis of a novel nano-sized fluoropolymer containing cadmium(II)-selective cavities by a new approach. According to the synthesis procedure, a newly synthesized luminescent complexing agent (5-((3-hydroxynaphthalen-2-yl)methylene)pyrimidine-2,4,6(1,3,5)-trione (HMPT)) was introduced to form a stable complex with Cd^{2+} ions. Then, the mixture of functional monomers and a cross-linker was added to the solution of the Cd(II)-HMPT complex formed and precipitation polymerization was carried out in an acetonitrile medium to produce a fluorescent imprinted polymer (FIP). The fluorescence signal of FIP was detected using a solid-state spectrofluorometer. To the best of our knowledge, there is no previous report on the synthesis of IIP based on ICT for the detection of Cd(II) in an aqueous medium.

Experimental

Reagents and instruments

Vinyl benzene and acryl amide (Merck, Germany) and ethylene glycol dimethacrylate (EGDMA) (Sigma-Aldrich, USA) were purified by distillation under reduced pressure. 2,2-(2-Methyl propionitrile) was obtained from (Arcos Organic, Geel, Belgium) and used as an initiator. $Cd(NO_3)_2 \cdot 4H_2O$ were from (Merck, Germany). Other chemicals were of analytical grade and were purchased from (Merck, Germany).

Vero cells were received from Blood Transfusion Research Centre, Tehran, Iran.

Fourier transform infrared (FT-IR) spectroscopic measurements were performed on a PerkinElmer Fourier transform infrared spectrometer. Thermogravimetric analysis was done by TGA Model Q50 V6.3 Build189. Scanning electron microscopy (SEM) images were obtained using a Model S4160 electron micro-scope (Hitachi). The fluorescence measurements were carried out on a PerkinElmer LS55 luminescence spectrometer. UV-Vis spectra were recorded in a UV-Vis Lambda 27 spectrophotometer (PerkinElmer).

Synthesis of 5-((3-hydroxynaphthalen-2-yl)methylene) pyrimidine-2,4,6(1,3,5)-trione

For the synthesis of 5-((3-hydroxynaphthalen-2-yl)methylene) pyrimidine-2,4,6(1,3,5)-trione (HMPT) acting as a complexing ligand for Cd^{2+}, 1 mmol of barbituric acid and 1 mmol of 3-hydroxy naphthalene 2-carbaldehyde were mixed together in 10 mL of NaOH (20% w/v). The mixture was then stirred for about 12 h. The completion of the reaction was checked by TLC. In order to precipitate the product, the mixture of reagents was diluted by HCl. After this, the crude product was purified by recrystallization.

Synthesis of nano-structured Cd(II)-imprinted polymer

For the preparation of the Cd-imprinted polymer by precipitation polymerization, 0.2 mmol of Cd $(NO_3)_2 \cdot 4H_2O$, was dissolved in 30 mL of acetonitrile. Then, 0.2 mmol of complexing agent was added to the solution. After this, 0.8 mmol of acryl amide and 0.4 mmol of vinyl benzene (as functional monomers) were gently added to the mixture while stirring. Subsequently, 4 mmol of EGDMA (as a cross-linker) and 25 mL of acetonitrile were added to the mixture. Finally, 0.01 g of AIBN (initiator) was transferred to the mixture. The mixture was purged with nitrogen for 15 min. The polymerization reaction was carried out in an oil bath fixed at 65 °C for 16 h. After reaction completion, the obtained polymer was separated and washed several times with EDTA solution (0.1 mol L^{-1}) and distilled water and dried at 60 °C. The non-imprinted polymer (NIP) was also synthesized using the same protocol except that Cd^{2+} ions were not present in the polymerization media. In order to gain small-sized IIP particles, the obtained powder was immersed in acetone and the supernatant particles were collected for final usage.

Fluorescence measurements

For all fluorescence studies, 1 μmol L^{-1} of ion solution in an aqueous medium was prepared. Then, 0.01 g of the IIP or NIP powder was added into the test tube containing metal ion solution fixed at a determined pH for a definite contact time. All the solutions of cadmium and other metal ions were prepared in double distilled water. After incubation of the polymer in the cadmium ion solution (or other metal ions), the polymer was separated from the solution and solid-state fluorescence spectra of the separated polymer powder were recorded utilizing the excitation wavelength of 356 nm.

Cytotoxicity assay

Cell viability in the presence of IIP was determined by means of the 3-(4,5-dimethylthiazol-2-yl)-2,5-diphenyltetrazolium bromide (MTT) assay. The MTT assay evaluates the number of living cells by reading the concentration of NAD(P)H-dependent

Open Access Article. Published on 24 January 2020. Downloaded on 2/11/2026 3:01:44 PM.
This article is licensed under a Creative Commons Attribution-NonCommercial 3.0 Unported Licence.

cellular oxido reductases. These enzymes reduce MTT to form insoluble formazan, which has a purple color. To achieve this goal, Vero cells were cultured in a Dulbecco's Modified Eagle Medium (DMEM) (10% fetal bovine serum, 2 mM glutamine, 100 U mL^{-1} penicillin, and 100 U mL^{-1} streptomycin, 95% air, 5% CO_2) and were incubated at 37 °C. For MTT assay, these cells were seeded in 96-well plates with 10^6 cells per mL and 100 μL per well. After 24 h, the cells were incubated with IIP (12.5–100 μg mL^{-1}) for 24 h in a cell culture medium. Afterward, MTT solution with 5 μg mL^{-1} and 20 μL per well was added. After 4 h, MTT was removed, and 100 μL DMSO was added to each well to dissolve the formed formazan. The absorbance was measured at 570 nm *via* a microplate reader. The cell viability, well-defined by the ratio of the absorbance in the absence of IIP to that in the presence of IIP, was thus obtained.

Recording of fluorescence image of cells in the presence of Cd-IP. Vero cells were cultured in DMEM. After 24 h, the IIP (50 μg mL^{-1}) was added to the cell culture dish, and the cells were incubated for another 48 h at 37 °C. Then, the cells were rinsed with PBS buffer solution (pH = 7.4) for three times to remove the residual polymer powder. The fluorescence images of Vero cells were acquired by an invert fluorescence microscope.

Result and discussion

Fluorescent ion imprinted polymer synthesis

The chemical structure of the newly synthesized ligand 5-((3-hydroxynaphthalen-2-yl)methylene)pyrimidine-2,4,6(1,3,5)-trione (HMPT) capable of forming a complex compound with Cd^{2+} is represented in Fig. 1, where the IIP synthesis route is also illustrated. It was found that this ligand could effectively interact with Cd^{2+} ions, leading to the formation of a complex of $[Cd(HMPT)_2]^{2+}$. Regarding the chemical structure of the ligand as well as the complex, vinyl benzene and acrylamide were selected as functional monomers to interact with naphthalene ring and amide functionalities, respectively, fixing the complex compound within the networked polymer (Fig. 1). The extraction of cadmium ions from the polymer resulted in the cavities being capable of selectively rebinding to the target ions. Due to the appropriate cadmium ion removal from the polymer, the ligands remained within the polymer, providing Cd^{2+}-selective sites.

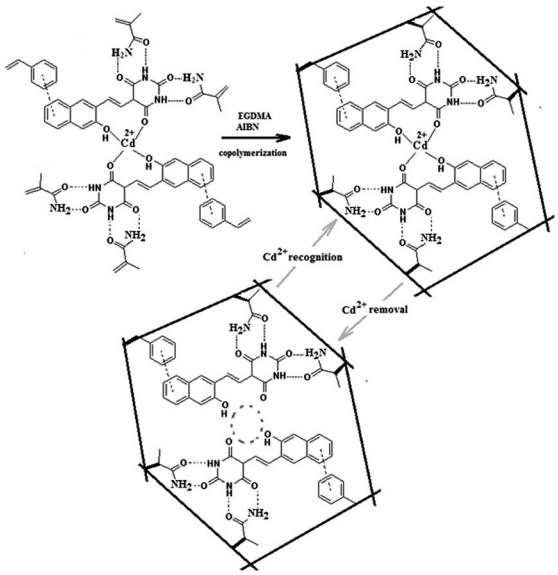

Fig. 1 Schematic representation of synthesis of IIP.

Characterization of the Cd^{2+}-imprinted polymer

Fig. 2 represents the Fourier transform infrared (FT-IR) spectra of HMPT, IIP, IIP-Cd^{2+}, NIP and reference polymer (R-polymer). R-polymer is the polymer synthesized in the absence of both HMPT and Cd^{2+}, whereas NIP is the polymer synthesized in the absence of Cd^{2+} and the presence of HMPT. The absorbance band at the wavenumber of ~1732 cm^{-1} present in all FT-IR spectra (Fig. 2) except in the FT-IR spectrum of HMPT is assigned to the carbonyl groups ($\nu_{C=O}$) of either the functional monomer (AA) or the cross-linker (EGDMA). The stretching frequency of the vinyl group, usually observed at ~1650 cm^{-1}, is absent in all polymer-related spectra, indicating that both monomers and cross-linker molecules are copolymerized. The stretching frequencies observed at ~1581 cm^{-1}, ~1565 cm^{-1} and ~1494 cm^{-1} in the FT-IR spectrum of IIP, IIP-Cd and NIP are attributed to the amide groups of the barbituric acid unit of the ligand (HMPT), clearly suggesting the presence of HMPT in all the networked polymers except R-polymer, which is synthesized without HMPT. In addition, twin IR bands situated at the wavenumbers of ~1000–1100 cm^{-1} and absorption band at ~2957 cm^{-1} observed for both IIP and NIP are assigned to the C–O stretching of HMPT and CH (sp^2) of HMPT and functional monomers, respectively. More importantly, the band at 1612 cm^{-1}, observed in the FT-IR spectrum of HMPT, is assigned to the carbonyl groups of the barbituric acid unit of the ligand. It seems that this peak shifts towards a lower frequency of about 1570 cm^{-1} in IIP-Cd^{2+}, which is attributed to the above-mentioned carbonyl group connected to Cd^{2+} *via* coordination

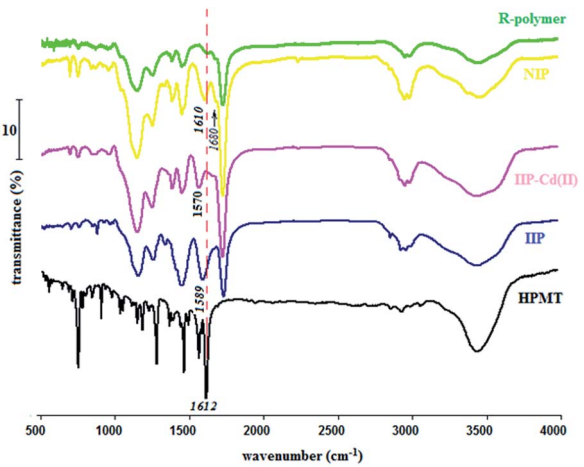

Fig. 2 FT-IR spectra of the ligand (HMPT), IIP, Cd^{2+}-loaded IIP (IIP-Cd(II)), NIP and reference polymer (R-polymer).

This journal is © The Royal Society of Chemistry 2020

Open Access Article. Published on 24 January 2020. Downloaded on 2/11/2026 3:01:44 PM.
This article is licensed under a Creative Commons Attribution-NonCommercial 3.0 Unported Licence.

bonding in the polymer. The removal of Cd^{2+} from the polymer, however, led to the return of the carbonyl peak of the ligand to about 1589 cm^{-1}, again confirming the ligand-Cd^{2+} interaction within the polymer cavities. Moreover, the position of the peak in this case suggests that without metal ions in the polymer, the ligand interacts with the functional monomers, leading to the weakening of the C=O group strength of the ligand. The inspection of the FT-IR spectrum of NIP shows that the carbonyl group stretching band related to HMPT is positioned at about 1610 cm^{-1}, which is partially coincident with that of HMPT, clearly confirming the above-mentioned statements. There is a band at about 1680 cm^{-1} in the FT-IR spectrum of NIP, which is absent in all other FT-IR spectra depicted in Fig. 2. This is likely related to the covalent attachment of the ligand to the polymer network in the absence of metal ions during the copolymerization reaction, the situation resulting in the synthesis of NIP. This will be discussed again in the next section in this article.

Thermogravimetric analysis (TGA) was also applied for the further evaluation of the fluorescent IIP (Fig. 3). As seen, there is some discrepancy between the TGA diagrams of IIP and NIP. Since after the removal of Cd^{2+} from the IIP polymer, its chemical structure would be similar to NIP, this difference suggests that the absence of metal ions in the polymer synthesis (NIP) leads to differences in the chemical structures of IIP and NIP. As mentioned before, an indication for such a phenomenon can be observed in the FT-IR spectrum of NIP.

The scanning electron microscopy image of IIP is illustrated in Fig. 4. The nano-structured polymeric particles can be seen in the image, suggesting a very high surface area for the IIP polymer.

Furthermore, the surface area and porosity of the synthesized IIP were evaluated *via* N_2 adsorption–desorption measurements. The Brunauer–Emmett–Teller (BET) and Barret–Joyner–Halenda (BJH) methods were applied to estimate the IIP specific surface area and pore diameter, respectively. Based on the described experiment, the surface area and average pore diameter of IIP were calculated to be about 238.4 $m^2\ g^{-1}$ and 7.3 nm, respectively.

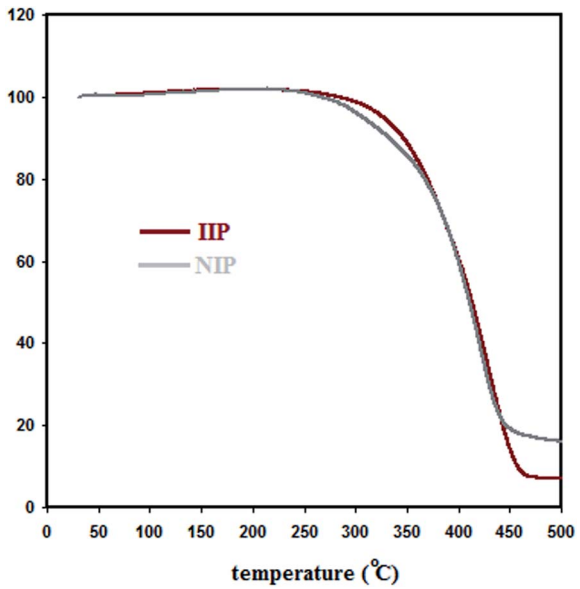

Fig. 3 Thermogravimetric analysis curves of IIP and NIP.

Fluorescence characteristics of the synthesized IIP/NIP and suggested mechanism

The fluorescence emission spectra of IIP and NIP in the presence and absence of Cd^{2+} ions were examined at the same concentration. As seen in Fig. 5, IIP exhibits a fluorescence peak at 440 nm in the absence of Cd^{2+} ions and NIP shows emission maxima at 515 nm. In view of the fact that HMPT exhibits its own fluorescence emission peak at about 435 nm (tested as its solution in acetonitrile) as well as based on the proof that both IIP and NIP contain HMPT as the fluorescence emitting agent, it can be concluded that the ligand entering IIP remains unchanged during the polymerization reaction; in contrast, HMPT used in the NIP preparation seems to be affected by the polymerization reaction condition and thus, it is likely to be involved in a chemical reaction responsible for polymer formation.

As can also be seen in the figure, upon Cd^{2+} ion addition (1 μM), the emission peak intensity of IIP at 440 nm decreases and a new emission peak appears at about 502 nm due to the plausible intramolecular charge transfer (ICT). However, no obvious change in the emission wavelength and fluorescence intensity is monitored after adding Cd^{2+} ions to NIP. This observation clearly shows that IIP can recognize Cd^{2+} ions and this recognition is manifested by the creation of a new fluorescence peak; however, no recognition event is assigned to the NIP synthesized herein as the blank polymer. Fig. 5(II) shows the appearance of IIP and NIP under visible (a) and ultraviolet (b) irradiation. As seen, there is a slight difference in the appearance of IIP and NIP under visible light; however, such a difference is highlighted when UV light is incident on the polymers. Interestingly, when contacting Cd^{2+} ions with the polymers, the colour of IIP completely changes, while that of NIP seems to be unchanged. This also is in accordance with the results depicted in the related fluorescence spectra.

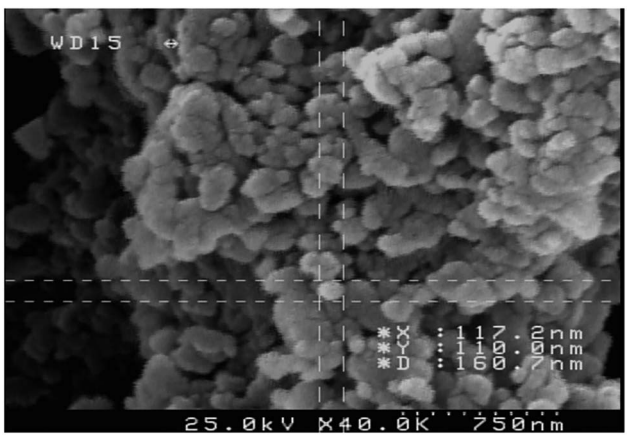

Fig. 4 The scanning electron microscopy image of the fluorescent Cd^{2+}-selective IIP.

Open Access Article. Published on 24 January 2020. Downloaded on 2/11/2026 3:01:44 PM.
This article is licensed under a Creative Commons Attribution-NonCommercial 3.0 Unported Licence.

We think that the HMPT ligand, utilized in the NIP polymer, connects to the polymer network *via* the OH group of hydroxynaphthalen-2-yl of HMPT during the radical polymerization reaction when the hydroxyl group forms an active radical capable of covalently attaching to the polymer structure. This gives rise to a distinct change in the chemical structure of the ligand in the resulting NIP material, thus leading to a bold shift in the polymer-connected ligand fluorescence compared to the fluorescence spectrum of the unchanged ligand (recorded separately in acetonitrile).

However, in the Cd^{2+}-imprinted polymer, the complexation of cadmium(II) ions with the OH group of hydroxynaphthalen-2-yl of HMPT prevents the involvement of the ligand in the described polymerization reaction, thus permitting the ligand to remain unchanged in IIP. Consequently, HMPT preserves its own nature.

This is confirmed by the similar fluorescence emission characteristics of the ligand entrapped in IIP ($\lambda_{max} = 440$ nm) and the ligand that did not enter the polymer ($\lambda_{max} = 435$ nm), as described in Fig. 5(I).

Based on the above-mentioned results, a possible sensing mechanism by IIP/NIP for the detection of Cd^{2+} is depicted in Fig. 5(III). After the addition of Cd^{2+} ions to IIP, it exhibited a "turn-on" response with high fluorescence intensity, following a pronounced spectral variation (red shift of about 65 nm). This may be due to the ICT process. However, other than the absence of cadmium ion recognition sites within NIP to accept metal ions, no ICT pathway is assigned to NIP since polymerization blocks the majority of the binding sites and thus, ICT is abrogated.

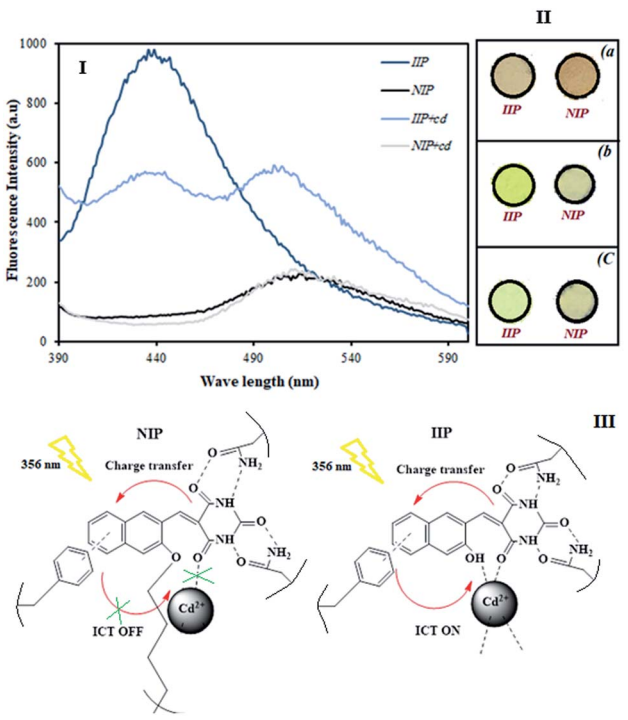

Fig. 5 Fluorescence emission spectra of the IIP and NIP before and after incubation in cadmium solution (1 μM) ($\lambda_{ex} = 356$ nm) (I); the appearance of the IIP and NIP under visible light (a) and under UV light ($\lambda_{ex} = 360$ nm) before (b) and after (c) incubation in cadmium solution (1×10^{-3} M) (II); probable mechanism for fluorescence response creation *via* ICT process in the IIP and NIP material (III).

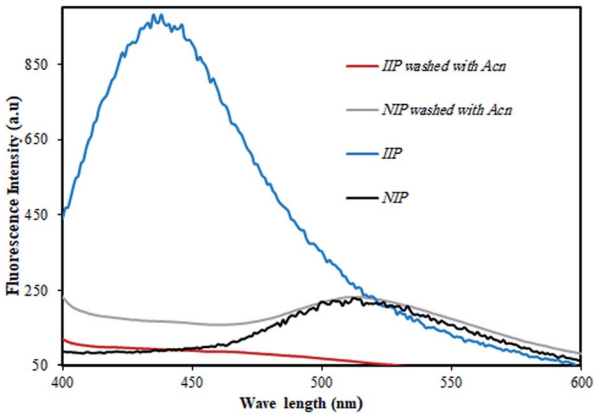

Fig. 6 Comparison of the fluorescence spectra of both IIP and NIP with those recorded for the same polymers after washing with acetonitrile, which is capable of removing the ligand from the polymer ($\lambda_{ex} = 356$ nm).

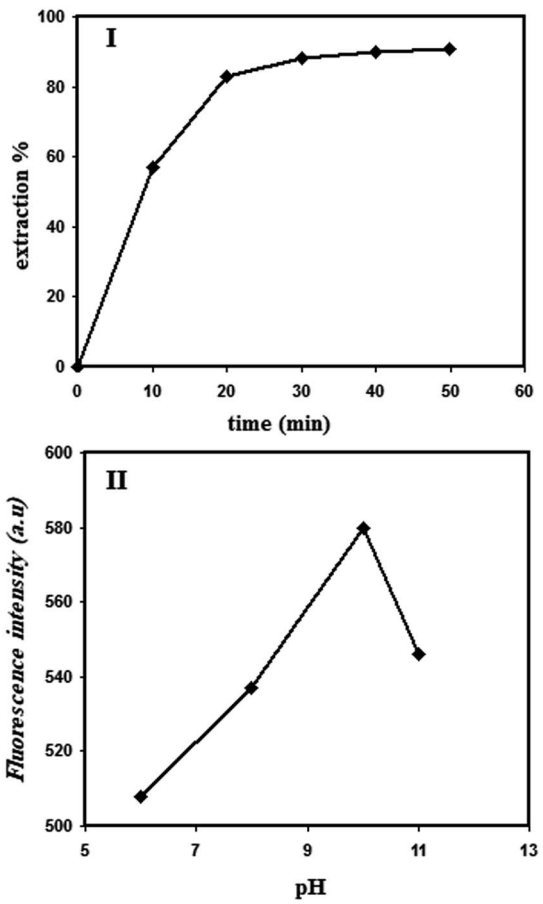

Fig. 7 The effect of polymer-cadmium solution contacting time (I) and cadmium solution pH on the fluorescence emission intensity of the ligand (II); $[Cd^{2+}] = 1$ μM; $\lambda_{ex} = 356$ nm; $\lambda_{em} = 502$ nm.

This journal is © The Royal Society of Chemistry 2020

Open Access Article. Published on 24 January 2020. Downloaded on 2/11/2026 3:01:44 PM.
This article is licensed under a Creative Commons Attribution-NonCommercial 3.0 Unported Licence.

In order to confirm the proposed mechanism, equal amounts of IIP and NIP were transferred to acetonitrile, which has the capability of properly dissolving HMPT. By this means, HMPT can be effectively removed from the polymer if it does not connect to the polymer *via* covalent bonding. To do this, the polymer dispersed in acetonitrile was stirred for about 20 min. In the next step, the solution was filtered and both the IIP and NIP powders were dried and prepared for fluorescence emission measurements. The results obtained are represented in Fig. 6. As can be seen, the fluorescence intensity of IIP is quenched totally after treating with acetonitrile due to the dissolving of HMPT in acetonitrile and thus its removal from the polymer network, while NIP preserves its own fluorescence intensity after treating with acetonitrile. This clearly indicated that the ligand inside NIP was not removed from the polymer due to the covalent attachment of the ligand to the polymer.

The effect of incubation time and pH on the adsorption of IIP

In order to investigate the adsorption kinetics of Cd^{2+} in IIP, a definite amount of the polymer powder was poured into the Cd^{2+} solution. The polymer was then separated from the solution after various incubation times. The Cd^{2+} contents of the solutions treated previously with IIP were then analyzed *via* ICP-OES and then, the extraction percent in IIP was calculated. The result is illustrated in Fig. 7(I). The figure shows that the Cd^{2+} adsorption in IIP enhances gradually on increasing the contact time and eventually at about 20 min, the adsorption/time curve reaches a plateau, indicating that a further increase in the adsorption time does not lead to a significant increase in Cd^{2+} extraction. Therefore, the extraction time of 20 min was chosen as the optimal condition for Cd^{2+} extraction in IIP. Moreover, the adsorption amount (Q) was calculated by the following equation:

$$Q = (C_0 - C_t) \times V/m \quad (1)$$

Here, C_0 and C_t are the initial and residual concentrations of Cd^{2+}, respectively; V is the volume of solution and m is the weight of the IIP material. From the equation, the adsorption amount (Q) was estimated by the value of 7.02 mg g^{-1}. The effect of pH on the fluorescence intensity of the IIP-Cd^{2+} material was

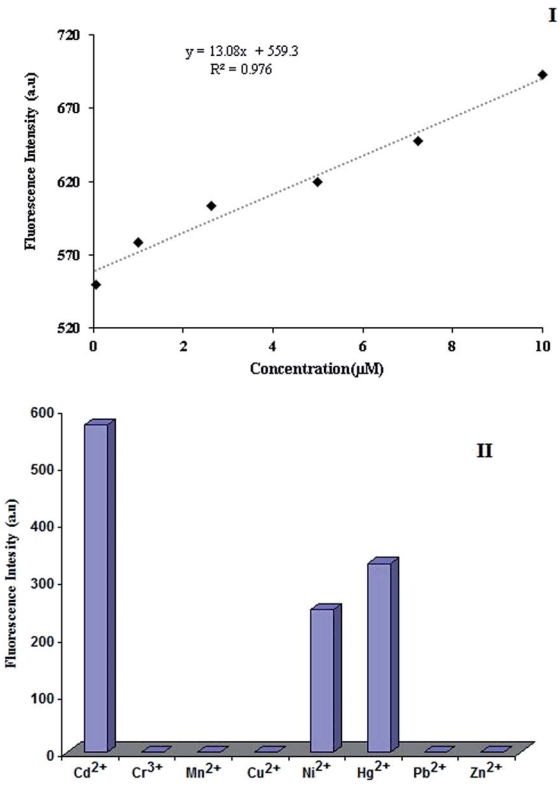

Fig. 8 Calibration curve obtained for the IIP-based fluorescent sensor; extraction pH = 10; extraction time = 20 min; IIP amount = 0.01 g; λ_{ex} = 356 nm; λ_{em} = 502 nm; comparison of fluorescence response intensities of the IIP to Cd^{2+} and various kinds of metal ions (the interference study) (II); metal ion concentration = 1 μM; λ_{ex} = 356 nm; λ_{em} = 502 nm.

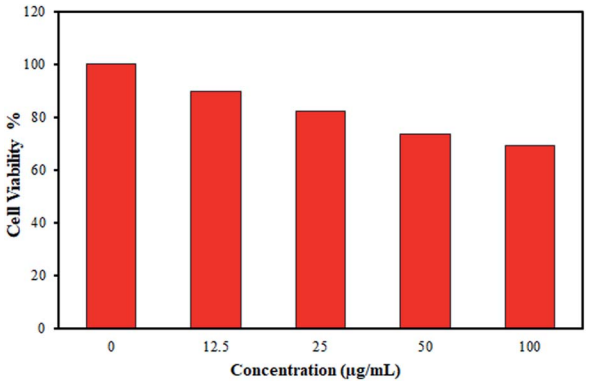

Fig. 9 Cell viability assay (MTT) of Vero cells in the presence of different amounts of IIP for 24 h; data represented are average of three replications.

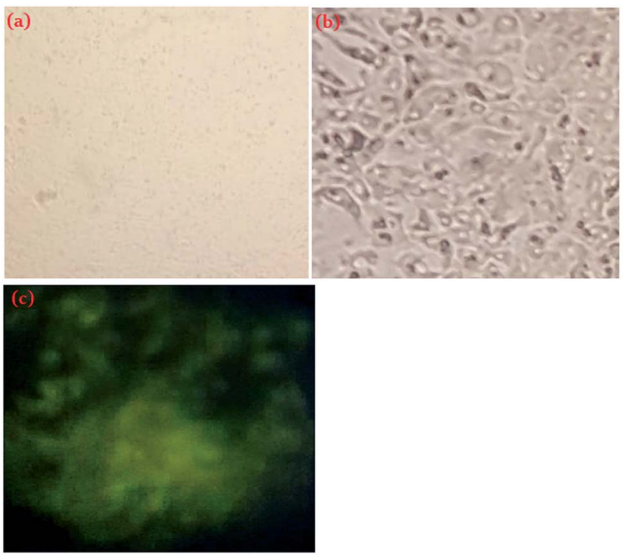

Fig. 10 Fluorescence microscopy images of Vero cell (a) and IIP-treated Vero cell (b) under visible light; the IIP-treated Vero cell under UV light (254 nm) (c).

Open Access Article. Published on 24 January 2020. Downloaded on 2/11/2026 3:01:44 PM.
This article is licensed under a Creative Commons Attribution-NonCommercial 3.0 Unported Licence.

Table 1 Comparison of the proposed chemosensor with some previously reported chemosensors

	Mechanism of detection	Linear dynamic range (μM)	LOD (nM)	Ref.
Cd^{2+}-fluorescent chemosensors	Fluorescence enhancement	0.25–2.5	29.3	45
	Fluorescence quenching	0.1–10	18.5	46
	Fluorescence enhancement	0–1.40	13.8	47
	Fluorescence quenching	7.2–10	2690	48
	Fluorescence enhancement	0.05–10	12.3	This work

also investigated. For this purpose, the IIP material was contacted with solutions containing a fixed concentration of Cd^{2+} and adjusted to various pH values. After a definite extraction time, the fluorescence intensity of the polymer separated from the solution was monitored at the wavelength of about 502 nm. As can be seen in Fig. 7(II), the fluorescence emission of IIP-Cd^{2+} is hugely influenced by pH. It seemed that the protonation of the acetylacetone group ($pK_a = 8.9$) of the barbituric acid part of the ligand at acidic as well as neutral conditions led to the weakening of the complexation of Cd^{2+} with the ligand entrapped in the Cd(II)-selective cavities of IIP, thus inhibiting the metal ion extraction in the polymer. Therefore, an alkaline medium provides the best situation for the interaction of the barbituric acid part of the ligand with Cd^{2+} ions, leading to the extraction of the ions to the polymer. However, highly alkaline conditions significantly diminish the IIP interaction with target ions because of the swelling of IIP and thus the loss of the polymer memory for the target metal ion Cd(II).

Solid-state fluorescence dependence of the IIP on Cd^{2+} concentration

The dependence of the fluorescence intensity of IIP on the Cd^{2+} ion concentration contacted with the polymer was checked *via* the solid-state fluorescence method. For this, the IIP material was contacted with various solutions containing various concentrations of Cd^{2+}. The calibration curve (Fig. 8(I)) suggests a good correlation between the solid-state fluorescence peak of IIP at the wavelength of 502 nm and the target ion concentration. The enhancement in the fluorescence intensity after Cd^{2+} chelation to IIP is attributed to the blocking of photoinduced electron transfer (PET) *via* metal ion (Cd^{2+}) coordination.

The fluorescence response of IIP to the other metal ions was also recorded and compared to that of Cd^{2+} in order to investigate the selectivity characteristic of the polymer. As illustrated in Fig. 8(II), the majority of the ions tested do not lead to a significant signal. Only Ni^{2+} and Hg^{2+} show a significant fluorescence signal after contacting with IIP. However, the sensitivity of the IIP material to cadmium ions is significantly higher than that for all other metal ions tested in this study.

Applicability of synthetic IIP in living cells

To validate the potential application of IIP in live cells, an assessment of the cell viability in the presence of the synthesized polymer (IIP) was performed by an MTT assay. As shown in Fig. 9, when IIP powder is incubated in Vero cells at the test concentrations from 12.5 to 100 μg mL^{-1}, all cell viabilities are more than about 70%, demonstrating that IIP has a minor cytotoxic effect on Vero cells (Fig. 9). Furthermore, Fig. 10(a) and (b) show the microscopy images of Vero cells under visible light before and after incubation with 50 μg L^{-1} IIP for 48 h, respectively. Before incubation with IIP, the Vero cells showed a non-fluorescence nature. However, after incubation with IIP for 48 h, the Vero cells showed intracellular green fluorescence under UV light (Fig. 10(c)). These observations suggest that the fluorescent imprinted polymer (IIP) with a nanometric size can enter the Vero cells and consequently, the imaging of live cells by means of IIP is possible. Additionally, by considering low LOQ (41 nM) and the adsorption capability of the as-prepared polymer that was primarily explored, the IIP material can be applied as a fluorescent tracer for intracellular cadmium ion detection.

Comparison of the proposed chemosensor with some previously reported chemosensors

The analytical characteristics and also the detection mechanism of the proposed IIP material as a turn-on chemosensor were compared to those of some previously reported fluorescent sensors reported for the determination of Cd^{2+} ions in aqueous media. The results are summarized in Table 1. This comparison demonstrates satisfactory results for the proposed probe.

Conclusion

A novel IIP material was introduced for the recognition and detection of Cd^{2+} in aqueous solutions *via* tracing the fluorescence intensity of the IIP material in the presence of Cd^{2+}. The IIP material exhibited a fluorescence emission peak at about 440 nm, which was similar to the ligand emission wavelength (435 nm). The contact of cadmium ions with the IIP material led to a significant decrease in the previous fluorescence signal (at 440 nm) and the generation of a new fluorescence peak at about 502 nm owing to the ICT mechanism. However, the NIP material exhibited a fluorescence signal centred at about 500 nm, which was not affected after contacting with Cd^{2+} ions. The IIP fluorescence signal of Cd^{2+} was found to be highly selective since none of the metal ions, namely, Cu^{2+}, Cr^{3+}, Mn^{2+}, Zn^{2+} and Pb^{2+} resulted in a fluorescence signal on IIP. The novel synthesized IIP material discussed in this study exhibits a new opportunity to effectively use a hydrophobic fluorescence ligand in an aqueous solution for metal ion determination. This can be

 This journal is © The Royal Society of Chemistry 2020

Open Access Article. Published on 24 January 2020. Downloaded on 2/11/2026 3:01:44 PM.
This article is licensed under a Creative Commons Attribution-NonCommercial 3.0 Unported Licence.

executed *via* the dispersion of the ligand-entrapped IIP powder in aqueous media, where the metal ion is extracted in the hydrophilic surface of IIP and interacts with the fluorescent ligand accommodated within the polymer. Moreover, it was shown that the polymer synthesized had a minor cytotoxic effect on Vero cells; thus, it can be used as a fluorescent probe for cadmium ion detection to intracellular goals.

Conflicts of interest

The authors declare that they have no conflict of interest.

Acknowledgements

The authors thank the University of Tehran for all supports.

References

1 S. E. Manahan, *Environmental Chemistry*, Lewis Publishers, Boca Raton, 6th edn, 1994.
2 J. S. Watson, *Separation Methods for Waste and Environmental Applications*, Marcel Dekker, New York, 1999.
3 M. M. Saeed and M. Ahmed, *Anal. Chim. Acta*, 2004, **525**, 289–292.
4 R. Bruce, *King (Editor-in-Chief)*, John Wiley & Sons, Chichester, 1994, p. 455.
5 T. Alizadeh, *Chin. J. Polym. Sci.*, 2011, **29**, 658–667.
6 S. A. Rezvani and A. Soleymanpour, *J. Chromatogr. A*, 2016, **1436**, 34–41.
7 A. Sixto, M. Fiedoruk-Pogrebniak, M. Rosende, D. Cocovi-Solberg, M. Knochen and M. Miro, *J. Anal. At. Spectrom.*, 2016, **31**, 473–481.
8 Q. Xu, W. Guo, L. Jin, Q. Guo and S. Hu, *J. Anal. At. Spectrom.*, 2016, **30**, 2010–2015.
9 J. Wu, Y. Hong, F. Guan, Y. Wang, Y. Tan, W. Yue, M. Wu, L. Bin, J. Wang and J. Wen, *Sci. Rep.*, 2016, 65.
10 M. J. Ahmed and U. K. Roy, *Turk. J. Chem.*, 2009, **33**, 709–726.
11 D. Yang, L. Wang, Z. Chen, M. Megharaj and R. Naidu, *Electrochim. Acta*, 2014, **132**, 223–229.
12 S. Hu, K. Wu, H. Yi, X. Dai and D. Cui, *Fresenius. J. Anal. Chem.*, 2001, **370**, 101–103.
13 T. Alizadeh, M. R. Ganjali, P. Nourozi, M. Zare and S. M. Hoseini, *J. Electroanal. Chem.*, 2011, **657**, 98–106.
14 C. Wardak, *Sens. Actuators, B*, 2015, **209**, 131–137.
15 J. Wang and Z. Song, Ultrasensitive determination of cadmium in rice by flow injection chemiluminescence analysis, *Food Anal. Methods*, 2014, **7**, 1671–1676.
16 Z. Li and L. Zhou, *J. Braz. Chem. Soc.*, 2008, **19**, 1347–1354.
17 A. Hafuka, A. Takitani, H. Suzuki, T. Iwabuchi, M. Takahashi, S. Okabe and H. Satoh, *Sensors*, 2017, **17**, 2291–22100.
18 H. N. Abdelhamid and H.-F. Wu, *RSC Adv.*, 2015, **5**, 50494–50504.
19 S. Guo, G. Liu, C. Fan and S. Pu, *RSC Adv.*, 2018, **8**, 22786–22798.
20 C. Lu, Z. Xu, J. Cui, R. Zhang and X. J. Qian, *Org. Chem.*, 2007, **72**, 3554–3557.
21 X. Tang, X. Peng, W. Dou, J. Mao, J. Zheng, W. Qin, W. Liu, J. Chang and X. Yao, *Org. Lett.*, 2008, **10**, 3653–3656.
22 M.-X. Huang, C.-H. Lv, Q.-D. Huang, J.-P. Lai and H. Sun, *RSC Adv.*, 2019, **9**, 36011–36019.
23 L. Xue, C. Liu and H. Jiang, *Org. Lett.*, 2009, **11**, 1655–1658.
24 K. Komatsu, K. Kikuchi, H. Kojima, Y. Urano and T. Nagano, *J. Am. Chem. Soc.*, 2005, **127**, 10197–10204.
25 E. M. Nolan, J. W. Ryu, J. Jaworski, R. P. Feazell, M. Sheng and S. J. Lippard, *J. Am. Chem. Soc.*, 2006, **128**, 15517–15528.
26 M. M. Henary, Y. G. Wu and C. J. Fahrni, *Chem.–Eur. J.*, 2004, **10**, 3015–3025.
27 M. De la Cruz-Guzman, A. Aguilar-Aguilar, L. Hernandez-Adame, A. Bañuelos-Frias, F. J. Medellín-Rodríguez and G. Palestino, *Nanoscale Res. Lett.*, 2014, **9**, 431–439.
28 H. He, J. Y. Liu and D. K. P. Ng, *J. Porphyrins Phthalocyanines*, 2013, **17**, 99–103.
29 Z. Lim, D. G. Smith, J. L. Kolanowski, R. L. Mattison, J. C. Knowles, S. Y. Baek, W. Chrzanowski and E. J. New, *J. R. Soc. Interface*, 2018, **15**, 0346.
30 M. Pamuk and F. Algi, *Tetrahedron Lett.*, 2012, **53**, 7010–7012.
31 Z. Miao, Y. Fu, Z. Xu, G. Li and J. Jiang, *Mendeleev Commun.*, 2009, **19**, 270–271.
32 P. Goswami and D. K. Das, *J. Fluoresc.*, 2012, **22**, 391–395.
33 T. Alizadeh and S. Amjadi, *New J. Chem.*, 2017, **41**, 4493–4502.
34 S. Wagner, J. Bell, M. Biyikal, K. Gawlitza and K. Rurack, *Biosens. Bioelectron.*, 2018, **99**, 244–250.
35 T. Alizadeh and S. Amjadi, *Microchim. Acta*, 2017, **184**, 2687–2695.
36 C. Xie, S. Wei, D. Chen, W. Lan, Z. Yan and Z. Wang, *RSC Adv.*, 2019, **9**, 23474–23483.
37 T. Alizadeh, N. Hamidi, M. R. Ganjali and F. Rafiei, *Microchim. Acta*, 2018, **185**, 16–23.
38 T. Alizadeh, F. Rafiei, N. Hamidi and M. R. Ganjali, *Electrochim. Acta*, 2017, **247**, 812–819.
39 T. Alizadeh and K. Atayi, *Mater. Chem. Phys.*, 2018, **209**, 180–187.
40 H. Wang, Y. Lin, Y. Li, A. Dolgormaa, H. Fang, L. Guo, J. Huang and J. Yang, *J. Inorg. Organomet. Polym.*, 2019, **29**, 1874–1885.
41 S. M. Ng and R. Narayanaswamy, *Anal. Bioanal. Chem.*, 2006, **386**, 1235–1244.
42 Z. Xu, P. Deng, J. Li and S. Tang, *Sens. Actuators, B*, 2018, **255**, 2095–2104.
43 P. E. Hande, A. B. Samui and P. S. Kulkarni, *Sens. Actuators, B*, 2017, **246**, 597–605.
44 O. Guney and F. C. Cebeci, *J. Appl. Polym. Sci.*, 2010, **117**, 2373–2379.
45 M.-X. Huang, C.-H. Lv, Q.-D. Huang, J.-P. Lai and H. Sun, *RSC Adv.*, 2019, **9**, 36011–36019.
46 P. Sakthivel, K. Sekar, G. Sivaraman and S. Singaravadivel, *J. Fluoresc.*, 2017, **27**, 1109–1115.
47 P. Wang, Y. An and Y. Liao, *Spectrochim. Acta, Part A*, 2019, **216**, 61–68.
48 Y. Tang, H. Liu, G. Jiang and Z. Gu, *J. Appl. Spectrosc.*, 2017, **84**, 911–914.